Electronic Supplementary Material (ESI) for Green Chemistry.

Supporting information

1. Detailed Description of Plasma Kinetic Model

The focus of this work was to investigate the different characteristics of N_2/H_2O plasma system to produce NH_3 in comparison to conventional N_2/H_2 system using 0D plasma kinetic model. The electron interactions, gas phase and surface interactions related to H_2O are included in addition to the original N_2/H_2 kinetic model.[1]

A new addition of gas phase reactions and surface reactions are shown in Table S1 and S2 respectively.

Table S1. Updates in gas phase reactions from original N_2/H_2 code [Hong et al.(2017)][1]; the gas temperature T_g and electron temperature T_e are in the unit of Kelvin [K]. M indicates any neutral if there is not given any specification.

	Process	Rate coefficient [cm^3s^{-1}] [cm^6s^{-1}]ǂ	Ref.
Excitation and ionization of H_2O, O_2, N_2O, NO by electron			
R1	$e + H_2O \rightarrow e + e + H_2O^+$	BOLSIG+*	2-42-42-42-4
R2	$e + O_2 \rightarrow e + e + O_2^+$	BOLSIG+	5, 6
R3	$e + NO \rightarrow e + e + NO^+$	BOLSIG+	7, 8
R5	$e + N_2O \rightarrow e + e + N_2O^+$	BOLSIG+	9
R6	$e + O_2 + M \rightarrow O_2^- + M$	BOLSIG+	3, 6
Dissociation reaction by electron			
R7	$e + H_2O \rightarrow OH + H + e$	BOLSIG+	7, 10
R8	$e + H_2O \rightarrow O^- + H_2$	BOLSIG+	7, 10
R9	$e + H_2O \rightarrow H + OH + e$	BOLSIG+	7, 10
R10	$e + H_2O \rightarrow O + H + H + e$	BOLSIG+	7, 10
R11	$e + H_2O \rightarrow H^+ + OH + e + e$	BOLSIG+	7, 10
R12	$e + O_2 \rightarrow O^- + O$	BOLSIG+	3, 6
R13	$e + O + O_2 \rightarrow O^- + O_2$	1×10^{-31}	11
R14	$e + O + O_2 \rightarrow O + O_2^-$	1×10^{-31}	11
R15	$e + O_3 \rightarrow O_2^- + O$	1×10^{-9}	11.
R16	$e + O_3 \rightarrow O^- + O_2$	1×10^{-11}	11
R17	$e + NO_2 \rightarrow O^- + NO$	1×10^{-11}	11
R18	$e + N_2O^+ \rightarrow N_2 + O$	$2.0\times10^{-7}(300/T_e)^{0.5}$	11
Ion-ion, ion-neutral interaction			
R19	$N_2^+ + O_2 \rightarrow O_2^+ + N_2$	$6\times10^{-11}*(300/T_{gas})^{0.5}$	12
R20	$N_2^+ + O \rightarrow NO^+ + N$	$1.3\times10^{-10}(300/T_{gas})^{0.5}$	12
R21	$N_2^+ + O \rightarrow O^+ + N_2$	$1.0\times10^{-11}(300/T_{gas})^{0.5}$	12
R22	$N_2^+ + O_3 \rightarrow O_2^+ + O + N_2$	1×10^{-10}	12
R23	$N_2^+ + N \rightarrow N^+ + N_2$	$7.2\times10^{-13}(T_{gas}/300)$	12
R24	$N_2^+ + NO \rightarrow NO^+ + N_2$	3.3×10^{-10}	12
R25	$N_2^+ + N_2O \rightarrow N_2O^+ + N_2$	5.0×10^{-10}	12
R26	$N_2^+ + N_2O \rightarrow NO^+ + N + N_2$	4.0×10^{-10}	12
R27	$O_2^+ + N_2 \rightarrow NO^+ + NO$	1.0×10^{-17}	12
R28	$O_2^+ + N \rightarrow NO^+ + O$	1.2×10^{-10}	12
R29	$O_2^+ + NO \rightarrow NO^+ + O_2$	6.3×10^{-10}	12
R30	$O_2^+ + NO_2 \rightarrow NO^+ + O_3$	1.0×10^{-11}	12
R31	$N_3^+ + O_2 \rightarrow O_2^+ + N + N_2$	2.3×10^{-11}	12

R32	$N_3^+ + NO \rightarrow NO^+ + N + N_2$	7.0×10^{-11}	12
R33	$N_3^+ + NO \rightarrow N_2O^+ + N_{2\times}$	7.0×10^{-11}	12
R34	$N_2O^+ + NO \rightarrow NO^+ + N_2O$	2.9×10^{-10}	12
R35	$N_4^+ + O_2 \rightarrow O_2^+ + 2N_2$	2.5×10^{-10}	12
R36	$N_4^+ + O \rightarrow O^+ + 2N_2$	2.5×10^{-10}	12
R37	$N_4^+ + NO \rightarrow NO^+ + 2N_2$	4×10^{-10}	12
R38	$O^- + N_2^+ \rightarrow N_2 + O$	3×10^{-6}	13
R39	$O^- + N^+ \rightarrow N + O$	3×10^{-6}	13
R40	$O^- + N_4^+ \rightarrow N_2 + N_2 + O$	3×10^{-6}	13
R41	$O^- + O_2^+ \rightarrow O_2 + O$	3×10^{-6}	13, 14
R42	$O^- + O^+ \rightarrow O + O$	3×10^{-6}	13
R43	$O^- + H_2O^+ \rightarrow H_2O + O$	3×10^{-6}	13, 14
R44	$O^- + O_2^+ \rightarrow O + O + O$	1×10^{-7}	11, 15
R45	$O^- + N_2^+ \rightarrow O + N + N$	1×10^{-7}	11, 15
R46	$O^- + H^+ \rightarrow H + O$	$2\times10^{-7}(T_{gas}/300)^{-0.5}$	15
R47	$O^- + H_2O^+ \rightarrow O + OH + H$	1×10^{-7}	15
R48	$O^- + O^+ + M \rightarrow O + O + M$	1.2×10^{-25}	13
R49	$O^- + N_2H^+ \rightarrow N_2H + O$	3×10^{-6}	ǂ
R50	$O^- + N_2^+ + M \rightarrow N_2O + M$	$2\times10^{-25}(300/T_{gas})^{2.5}$	12
R51	$O_2^- + N_2^+ \rightarrow N_2 + O_2$	2×10^{-6}	13, 16
R52	$O_2^- + N_2^+ \rightarrow O_2 + N + N$	1×10^{-7}	12
R53	$O_2^- + N^+ \rightarrow O_2 + N$	2×10^{-6}	13, 14
R54	$O_2^- + N_4^+ \rightarrow O_2 + N_2 + N_2$	2×10^{-6}	13
R55	$O_2^- + O_2^+ \rightarrow O_2 + O_2$	2×10^{-6}	13, 14
R56	$O_2^- + N_2H^+ \rightarrow O_2 + N_2H$	2×10^{-6}	ϕ
R57	$O_2^- + N_2H^+ \rightarrow O_2 + N_2 + H$	2×10^{-6}	ϕ
R58	$O_2^- + O^+ \rightarrow O_2 + O$	2×10^{-6}	13, 14
R59	$O_2^- + H_2O^+ \rightarrow O_2 + H_2O$	2×10^{-6}	13, 14
R60	$O_2^- + H^+ \rightarrow O_2 + H$	$2\times10^{-7}(T_{gas}/300)^{-0.5}$	15
R61	$O_2^- + N_2 \rightarrow O_2 + N_2 + e$	$1.9\times10^{-12}(T_{gas}/300)^{0.5}\exp(^-4990/T_{gas})$	12
R62	$O_2^- + O_2 \rightarrow O_2 + O_2 + e$	$2.7\times10^{-10}(T_{gas}/300)^{0.5}\exp(^-5590/T_{gas})$	12
R63	$O^- + O_2 \rightarrow O_3 + e$	5×10^{-15}	12
R64	$O_2^- + N_2(A3) \rightarrow O_2 + N_2 + e$	2.1×10^{-9}	12
R65	$O_2^- + N_2(B3) \rightarrow O_2 + N_2 + e$	2.5×10^{-9}	12
R66	$O^- + N_2(A3) \rightarrow O + N_2 + e$	2.2×10^{-9}	12
R67	$O^- + N_2(B3) \rightarrow O + N_2 + e$	1.9×10^{-9}	12
R68	$O_2^- + O \rightarrow O_3 + e$	1.5×10^{-10}	12
R69	$O_2^- + N \rightarrow NO_2 + e$	5.0×10^{-10}	12
R70	$O^- + O \rightarrow O_2 + e$	5.0×10^{-10}	10, 17
R71	$O^- + N \rightarrow NO + e$	2.6×10^{-10}	12
R72	$O^- + NO \rightarrow NO_2 + e$	2.6×10^{-10}	12
R73	$NH_2^+ + H_2O \rightarrow NH_4^+ + O$	1.0×10^{-10}	12
R74	$NH_3^+ + H_2O \rightarrow NH_4^+ + OH$	3×10^{-11}	12
R75	$N_4^+ + H_2O \rightarrow H_2O^+ + 2N_2$	3×10^{-9}	12

Vibrational excitation and de-excitation of H_2O molecules			
R76	$e + H_2O \rightleftarrows e + H_2O(\nu_i)$	BOLSIG+ (Symmetric stretch (100) ν_1 3656.65 cm^{-1}, Bend(010) ν_2 1594.59 cm^{-1}, Anti-symmetric stretch(001) ν_3 3755.79cm^{-1})[19] T	[3]
V-T interaction between $N_2((\nu_i)$ and ground state H_2O			
R77	$N_2(\nu_i) + H_2O \rightleftarrows N_2(\nu_{i-1}) + H_2O$	Equation S1	[12]
Neutral-neutral chemical reactions			
R78	$H_2O + M \rightarrow OH + H + M$	$5.9\times10^{-7}(T_{gas}/300)^{-2.2}exp(-59000/T_{gas})$	[12]
R79	$OH + H + M \rightarrow H_2O + M$	$6.7\times10^{-31}(T_{gas}/300)^{-2}$	[12]
R80	$H_2 + M \rightarrow 2H + M$	$3.7\times10^{-10}exp(-48300/T_{gas})$	[12]
R81	$2H + M \rightarrow H_2 + M$	$8.3\times10^{-33}(T_{gas}/300)^{-1}$	[12]
R82	$OH + M \rightarrow H + O + M$	$4.7\times10^{-8}(T_{gas}/300)^{-1}exp(-50830/T_{gas})$	[12]
R83	$H + O + M \rightarrow OH + M$	$6.5\times10^{-32}(T_{gas}/300)^{-1}$	[12]
R84	$O_2 + H \rightarrow OH + O$	$3.7\times10^{-10}exp(-8455/T_{gas})$	[12]
R85	$OH + O \rightarrow O_2 + H$	$2.2\times10^{-11}exp(-350/T_{gas})$	[12]
R86	$H_2 + O \rightarrow OH + H$	$9\times10^{-12}(T_{gas}/300)exp(-4480/T_{gas})$	[12]
R87	$OH + H \rightarrow H_2 + O$	$4.1\times10^{-12}(T_{gas}/300)exp(-3500/T_{gas})$	[12]
R88	$H_2O + H \rightarrow OH + H_2$	$1.4\times10^{-10}exp(-10116/T_{gas})$	[12]
R89	$OH + H_2 \rightarrow H_2O + H$	$3.2\times10^{-11}exp(-2600/T_{gas})$	[12]
R90	$H_2O + O \rightarrow 2OH$	$9.6\times10^{-11}exp(-9059/T_{gas})$	[12]
R91	$OH + OH \rightarrow H_2O + O$	$8.8\times10^{-12}exp(-503/T_{gas})$	[12]
R92	$H_2 + O_2 \rightarrow 2OH$	$2.8\times10^{-9}exp(-24200/T_{gas})$	[12]
R93	$OH + OH \rightarrow H_2 + O_2$	$2.8\times10^{-11}exp(-24100/T_{gas})$	[12]
R94	$HO_2 + M \rightarrow H + O_2 + M$	$3.5\times10^{-9}exp(-23000/T_{gas})$	[12]
R95	$H + O_2 + M \rightarrow HO_2 + M$	$4.1\times10^{-33}exp(-500/T_{gas})$	[12]
R96	$H_2 + O_2 \rightarrow H + HO_2$	$3.2\times10^{-11}exp(-24100/T_{gas})$	[12]
R97	$H + HO_2 \rightarrow H_2 + O_2$	2.2×10^{-11}	[12]
R98	$H_2O + O \rightarrow H + HO_2$	$2.8\times10^{-12}(T_{gas}/300)^{0.37}exp(-28743/T_{gas})$	[12]
R99	$H + HO_2 \rightarrow H_2O + O$	$1.7\times10^{-11}exp(-540/T_{gas})$	[12]
R100	$H_2O + O_2 \rightarrow OH + HO_2$	$4.3\times10^{-9}(T_{gas}/300)^{0.5}exp(-36600/T_{gas})$	[12]
R101	$OH + HO_2 \rightarrow H_2O + O_2$	5.0×10^{-10}	[12]
R102	$H_2O + OH \rightarrow H_2 + HO_2$	$1.4\times10^{-13}exp(-36100/T_{gas})$	[12]
R103	$H_2 + HO_2 \rightarrow H_2O + OH$	$1.1\times10^{-12}exp(-9400/T_{gas})$	[12]
R104	$OH + OH \rightarrow H + HO_2$	$2.0\times10^{-11}exp(-20200/T_{gas})$	[12]
R105	$H + HO_2 \rightarrow OH + OH$	$4.2\times10^{-10}exp(-950/T_{gas})$	[12]
R106	$OH + O_2 \rightarrow O + HO_2$	$2.2\times10^{-11}exp(-28200/T_{gas})$	[12]
R107	$O + HO_2 \rightarrow OH + O_2$	$8.3\times10^{-11}exp(-500/T_{gas})$	[12]
R108	$HO_2 + HO_2 \rightarrow H_2O_2 + O_2$	$3.0\times10^{-11}exp(-500/T_{gas})$	[12]
R109	$H_2O_2 + O_2 \rightarrow HO_2 + HO_2$	$5.0\times10^{-11}exp(-21600/T_{gas})$	[12]
R110	$HO_2 + H_2O \rightarrow H_2O_2 + OH$	$3.0\times10^{-11}exp(-15100/T_{gas})$	[12]
R111	$H_2O_2 + OH \rightarrow HO_2 + H_2O$	$1.7\times10^{-11}exp(-910/T_{gas})$	[12]
R112	$OH + HO_2 \rightarrow H_2O_2 + O$	$1.5\times10^{-12}(T_{gas}/300)^{0.5}exp(-44800/T_{gas})$	[12]
R113	$H_2O_2 + O \rightarrow OH + HO_2$	$1.4\times10^{-12}exp(-2130/T_{gas})$	[12]
R114	$N_2H + O \rightarrow N_2 + OH$	$1.7\times10^{-11}exp(-2500/T_{gas})$	[12]

R115	$N_2H + O \rightarrow N_2O + H$	$1.7\times10^{-11}\exp(^{-}1500/T_{gas})$	12
R116	$N_2O + H \rightarrow N_2H + O$	$7.1\times10^{-8}\exp(^{-}23380/T_{gas})$	12
R117	$N_2H + OH \rightarrow N_2 + H_2O$	5.2×10^{-11}	12
R118	$N_2 + H_2O \rightarrow N_2H + OH$	$7.6\times10^{-11}\exp(^{-}64510/T_{gas})$	12
R119	$N_2H + O_2 \rightarrow N_2 + HO_2$	$1.7\times10^{-11}\exp(^{-}2020/T_{gas})$	12
R120	$N_2 + HO_2 \rightarrow N_2H + O_2$	$5.8\times10^{-11}\exp(^{-}29230/T_{gas})$	12
R121	$NO + NH \rightarrow N_2O + H$	$1.7\times10^{-12}\exp(^{-}250/T_{gas})$	12
R122	$N_2O + H \rightarrow NO + NH$	$4.5\times10^{-10}\exp(^{-}15020/T_{gas})$	12
R123	$N_2(A3) + O_2 \rightarrow N_2O + O$	$2.0\times10^{-14}(T_{gas}/300)^{0.55}$	19
R124	$N_2(A3) + N_2O \rightarrow N_2 + N + NO$	1.0×10^{-11} ǂ	19
R125	$N_2(a`1) + NO \rightarrow N_2 + N + O$	3.6×10^{-11}	19
R126	$N_2(C3) + O_2 \rightarrow N_2 + O + O$	3.0×10^{-10}	19
R127	$N_2(a`1) + O_2 \rightarrow N_2 + O + O$	2.8×10^{-11}	19
R128	$O + M \rightarrow NO + N$	Equation S2* for $M = N_2(X)$, $N_2(\nu_i)$	12
R129	$N(2D) + O_2 \rightarrow NO + O$	$6\times10^{-12}(T_{gas}/300)^{0.5}$	11
R130	$N(2P) + O_2 \rightarrow NO + O$	2.6×10^{-12}	11
R131	$N(2D) + NO \rightarrow N_2O$	6×10^{-11}	11
R132	$N(2D) + NO \rightarrow N_2 + O$	1.8×10^{-10}	11
R133	$N(2D) + N_2O \rightarrow NO + N_2$	3×10^{-12}	11
R134	$N(2D) + N_2 \rightarrow N + N_2$	6×10^{-15}	11
R135	$N(2P) + NO \rightarrow N_2(A3) + O$	3.4×10^{-11}	11
R136	$N(2P) + NO \rightarrow N_2 + O$	3.0×10^{-11}	11
R137	$N(2P) + N_2 \rightarrow N(2D) + N_2$	2×10^{-18}	11
R138	$N(2P) + N \rightarrow N(2D) + N$	1.8×10^{-12}	11
R139	$NH_3 + O \rightarrow NH_2 + OH$	$3.3\times10^{-11}\exp(^{-}4470/T_{gas})$	12
R140	$NH_2 + OH \rightarrow NH_3 + O$	$1.4\times10^{-12}\exp(^{-}1360/T_{gas})$	12
R141	$NH_2 + O \rightarrow NH + OH$	$9.6\times10^{-12}(T_{gas}/300)^{-0.5}$	12
R142	$NH + OH \rightarrow NH_2 + O$	$3.0\times10^{-12}(T_{gas}/300)^{-0.5}\exp(^{-}7360/T_{gas})$	12
R143	$NH_2 + O \rightarrow HNO + H$	$6.1\times10^{-11}(T_{gas}/300)^{-0.5}$	12
R144	$HNO + H \rightarrow NH_2 + O$	$3.6\times10^{-10}(T_{gas}/300)^{-0.5}\exp(^{-}14160/T_{gas})$	12
R145	$HNO + N \rightarrow NO + NH$	$1.7\times10^{-11}\exp(^{-}1000/T_{gas})$	12
R146	$NO + NH \rightarrow HNO + N$	$2.1\times10^{-12}\exp(^{-}18500/T_{gas})$	12
R147	$NH_2 + NO \rightarrow N_2 + H_2O$	$6.7\times10^{-11}(T_{gas}/300)^{-2.5}\exp(^{-}960/T_{gas})$	12
R148	$N_2 + H_2O \rightarrow NH_2 + NO$	$2\times10^{-9}(T_{gas}/300)^{-2.5}\exp(^{-}64110/T_{gas})$	12
R149	$NO_2 + NH \rightarrow HNO + NO$	$2.9\times10^{-12}(T_{gas}/300)^{0.5}\exp(^{-}2020/T_{gas})$	12
R150	$HNO + NO \rightarrow NO_2 + NH$	$1.6\times10^{-12}(T_{gas}/300)^{0.5}\exp(^{-}24040/T_{gas})$	12
R151	$N_2O + NH \rightarrow N_2 + HNO$	$3.3\times10^{-12}\exp(^{-}3000/T_{gas})$	12
R152	$NH_2 + O_2 \rightarrow HNO + OH$	$2.9\times10^{-12}\exp(^{-}7560/T_{gas})$	12
R153	$HNO + OH \rightarrow NH_2 + O_2$	$1.8\times10^{-12}\exp(^{-}13360/T_{gas})$	12
R154	$NH_2 + O_2 \rightarrow NH + HO_2$	$1.7\times10^{-10}\exp(^{-}25200/T_{gas})$	12
R155	$NH + HO_2 \rightarrow NH_2 + O_2$	$5.5\times10^{-11}\exp(^{-}2750/T_{gas})$	12
R156	$NH + O_2 \rightarrow HNO + O$	$1.7\times10^{-12}\exp(^{-}1610/T_{gas})$	12
R157	$HNO + O \rightarrow NH + O_2$	$4.1\times10^{-12}\exp(^{-}5280/T_{gas})$	12
R158	$NH + O \rightarrow N + OH$	$1.8\times10^{-11}(T_{gas}/300)^{0.5}\exp(^{-}4000/T_{gas})$	12
R159	$N + OH \rightarrow NH + O$	$3.7\times10^{-11}(T_{gas}/300)^{0.5}\exp(^{-}17840/T_{gas})$	12

R160	$NH + O \rightarrow NO + H$	$1.8\times10^{-11}(T_{gas}/300)^{0.5}$	12
R161	$NO + H \rightarrow NH + O$	$1.0\times10^{-10}(T_{gas}/300)^{0.5}exp(^{-}38010/T_{gas})$	12
R162	$NH_3 + OH \rightarrow NH_2 + H_2O$	$9.5\times10^{-11}exp(^{-}4055/T_{gas})$	12
R163	$NH_2 + H_2O \rightarrow NH_3 + OH$	$5.0\times10^{-11}exp(^{-}9680/T_{gas})$	12
R164	$NH_2 + OH \rightarrow NH + H_2O$	$1.4\times10^{-11}(T_{gas}/300)^{0.5}exp(^{-}1000/T_{gas})$	12
R165	$NH + H_2O \rightarrow NH_2 + OH$	$4.9\times10^{-11}(T_{gas}/300)^{0.5}exp(^{-}17090/T_{gas})$	12
R166	$NH + OH \rightarrow N + H_2O$	$1.4\times10^{-11}(T_{gas}/300)^{0.5}exp(^{-}1000/T_{gas})$	12
R167	$N + H_2O \rightarrow NH + OH$	$3.0\times10^{-}{}_{9}(T_{gas}/300)^{0.5}exp(^{-}23370/T_{gas})$	12
R168	$HNO + H \rightarrow NH + OH$	$5.8\times10^{-10}(T_{gas}/300)^{0.5}exp(^{-}12720/T_{gas})$	12
R169	$NH + OH \rightarrow HNO + H$	$2.9\times10^{-11}(T_{gas}/300)^{0.5}exp(^{-}1010/T_{gas})$	12
R170	$H_2O + O_2 \rightarrow H_2O_2 + O$	$9.8\times10^{-8}(T_{gas}/300)^{0.5}exp(^{-}44800/T_{gas})$	12
R171	$H_2O_2 + O \rightarrow H_2O + O_2$	$1.4\times10^{-12}exp(^{-}2130/T_{gas})$	12
R172	$H + H_2O_2 \rightarrow H_2O + OH$	$8.3\times10^{-10}exp(^{-}5000/T_{gas})$	12
R173	$H_2O + OH \rightarrow H + H_2O_2$	$4.0\times10^{-10}exp(^{-}40500/T_{gas})$	12
R174	$O + NO + N_2 \rightarrow NO_2 + N_2$	$1.2\times10^{-31}(300/T_{gas})^{1.8}$	12
R175	$O + NO + NO \rightarrow NO_2 + NO$	$0.78*1.2\times10^{-31}(300/T_{gas})^{1.8}$	12
R176	$O + NO + O_2 \rightarrow NO_2 + O_2$	$0.78*1.2\times10^{-31}(300/T_{gas})^{1.8}$	12
R177	$O + NO_2 + N_2 \rightarrow NO_3 + N_2$	$8.9\times10^{-32}(300/T_{gas})^{2}$	12
R178	$O + NO_2 + NO \rightarrow NO_3 + NO$	$2.4*8.9\times10^{-32}(300/T_{gas})^{2}$	12
R179	$O + NO_2 + O_2 \rightarrow NO_3 + O_2$	$8.9\times10^{-32}(300/T_{gas})^{2}$	12
R180	$NO_2 + N_2 \rightarrow NO + O + N_2$	$6.8\times10^{-6}(300/T_{gas})^{2}exp(^{-}36180/T_{gas})$	12
R181	$NO_2 + O_2 \rightarrow NO + O + O_2$	$0.78\times6.8\times10^{-6}(300/T_{gas})^{2}exp(^{-}36180/T_{gas})$	12
R182	$NO_2 + NO \rightarrow NO + O + NO$	$7.8\times6.8\times10^{-6}(300/T_{gas})^{2}exp(^{-}36180/T_{gas})$	12
R183	$NO_2 + NO_2 \rightarrow NO + O + NO_2$	$5.9\times6.8\times10^{-6}*(300/T_{gas})^{2}exp(^{-}36180/T_{gas})$	12
R184	$N + NO \rightarrow O + N_2$	$1.8\times10^{-11}(T_{gas}/300)^{0.5}$	12
R185	$N + O_2 \rightarrow O + NO$	$3.2\times10^{-12}(T_{gas}/300)exp(^{-}3150/T_{gas})$	12
R186	$N + NO_2 \rightarrow 2O + N_2$	9.1×10^{-13}	12
R187	$N + NO_2 \rightarrow O + N_2O$	3×10^{-12}	12
R188	$N + NO_2 \rightarrow N_2 + O_2$	7×10^{-13}	12
R189	$N + NO_2 \rightarrow NO + NO$	2.3×10^{-12}	12
R190	$O + NO \rightarrow NO_2 + \gamma$	4.2×10^{-18}	12
R191	$O + NO_2 \rightarrow NO + O_2$	$9.1\times10^{-12}(T_{gas}/300)^{0.18}$	12
R192	$O + NO_3 \rightarrow O_2 + NO_2$	1×10^{-11}	12
R193	$N_2 + O_2 \rightarrow O + N_2O$	$2.5\times10^{-10}exp(^{-}50390/T_{gas})$	12
R194	$NO + NO \rightarrow N + NO_2$	$3.3\times10^{-16}(300/T_{gas})^{0.5}exp(^{-}39200/T_{gas})$	12
R195	$NO + NO \rightarrow O + N_2O$	$2.2\times10^{-12}(300/T_{gas})^{0.5}exp(^{-}32100/T_{gas})$	12
R196	$NO + O_2 \rightarrow O + NO_2$	$2.8\times10^{-12}exp(^{-}23400/T_{gas})$	12
R197	$NO + NO_3 \rightarrow NO_2 + NO_2$	1.7×10^{-11}	12
R198	$NO_2 + NO_2 \rightarrow 2NO + O_2$	$3.3\times10^{-12}exp(^{-}13500/T_{gas})$	12
R199	$NO_2 + NO_3 \rightarrow NO + NO_2 + O_2$	$2.3\times10^{-13}exp(^{-}1600/T_{gas})$	12
R200	$NO_3 + M \rightarrow NO_2 + O + M$	$k_{R200}=3.1\times10^{-5}(300/T_{gas})^{2}exp(^{-}25000/T_{gas})$ $M = N_2, O_2, NO$ $10\times k_{R200}$, $M = N, O$	12

R201	$NO_3 + M \rightarrow NO + O_2 + M$	$k_{R201} = 6.2\times10^{-5}(300/T_{gas})^2\exp(^-25000/T_{gas})$ M = N_2, O_2, NO	12
		12× k_{R201}, M = N, O	
R202	$NO_3 + OH \rightarrow HO_2 + NO_2$	2.6×10^{-11}	12
R203	$NO_3 + HO_2 \rightarrow NO_2 + OH + O_2$	3.6×10^{-12}	12
R204	$O + N_2 + M \rightarrow N_2O + M$	$3.9\times10^{-35}\exp(^-10400/T_{gas})$	12
R205	$N_2O + M \rightarrow N_2 + O + M$	$1.2\times10^{-8}(300/T_{gas})\exp(^-29000/T_{gas})$	12
R206	$N_2O + OH \rightarrow N_2 + HO_2$	$1.0\times10^{-12}\exp(^-5000/T_{gas})$	12
R207	$N_2O + H \rightarrow N_2 + OH$	$1.3\times10^{-10}\exp(^-7600/T_{gas})$	12
R208	$N_2 + OH \rightarrow N_2O + H$	$4.2\times10^{-12}\exp(^-39967/T_{gas})$	12
R209	$N_2 + HO_2 \rightarrow N_2O + OH$	$1.2\times10^{-12}\exp(^-20160/T_{gas})$	12
R210	$NH_2 + NO \rightarrow N_2O + H_2$	$8.3\times10^{-11}\exp(^-12450/T_{gas})$	12
R211	$N_2O + H_2 \rightarrow NH_2 + NO$	$6.9\times10^{-9}\exp(^-34520/T_{gas})$	12
R212	$NH_2 + NO_2 \rightarrow N_2O + H_2O$	$2.67\times10^{-8}(T_{gas}/300)^{-1.4}\exp(^-135/T_{gas})$	20
R213	$N_2O + O \rightarrow NO + NO$	$1.5\times10^{-10}\exp(^-14090/T_{gas})$	12
R214	$N + O + M \rightarrow NO + M$	$1.8\times10^{-31}(300/T_{gas})$, M= N, O, NO	12
		$1\times10^{-32}(300/T_{gas})^{0.5}$ for the rest neutrals	
R215	$O + O + N_2 \rightarrow O_2 + N_2$	$2.8\times10^{-34}\exp(720/T_{gas})$	12
R216	$O + O + O_2 \rightarrow O_2 + O_2$	$4.0\times10^{-33}(300/T_{gas})^{0.41}$	12
R217	$O + O + O \rightarrow O_2 + O$	$3.6\times4.0\times10^{-33}(300/T_{gas})^{0.41}$	12
R218	$O + O + N \rightarrow O_2 + N$	$0.8\times4.0\times10^{-33}(300/T_{gas})^{0.41}$	12
R219	$O + O + NO \rightarrow O_2 + NO$	$0.17\times4.0\times10^{-33}(300/T_{gas})^{0.41}$	12
R220	$O_2 + M \rightarrow O + O + M$	$k_{R221} = 6.1\times10^{-9}(1^-\exp(^-2240/T_{gas}))\exp(^-59380/T_{gas})$ M= N_2, NO, N	12
		5.9× k_{R221}, M= O_2	
		21× k_{R221}, M= O	
R221	$O + HNO_2 \rightarrow O_2 + HNO$	$5\times10^{-12}\exp(^-8000/T_{gas})$	12
R222	$HNO + O \rightarrow NO + OH$	$1.4\times10^{-11}(300/T_{gas})^{0.5}\exp(^-1000/T_{gas})$	12
R223	$NO + OH \rightarrow HNO + O$	$3.4\times10^{-12}(300/T_{gas})^{0.5}\exp(^-27468/T_{gas})$	12
R224	$HNO + OH \rightarrow NO + H_2O$	$3.6\times10^{-11}(300/T_{gas})^{0.5}\exp(^-1000/T_{gas})$	12
R225	$NO + H_2O \rightarrow HNO + OH$	$7.4\times10^{-11}(300/T_{gas})^{0.5}\exp(^-36338/T_{gas})$	12
R226	$NO + HO_2 \rightarrow O_2 + HNO$	$3.3\times10^{-13}\exp(^-1000/T_{gas})$	12
R227	$HNO + HO_2 \rightarrow NO + H_2O_2$	$9.1\times10^{-12}(300/T_{gas})^{0.5}\exp(^-1000/T_{gas})$	12
R228	$NO + H_2O_2 \rightarrow HNO + HO_2$	$1.1\times10^{-12}(300/T_{gas})^{0.5}\exp(^-18468/T_{gas})$	12
R229	$HNO + H \rightarrow NO + H_2$	$2.1\times10^{-11}\exp(^-2000/T_{gas})$	12
R230	$NO + H_2 \rightarrow HNO + H$	$9.1\times10^{-12}\exp(^-29686/T_{gas})$	12
R231	$HNO + M \rightarrow H + NO + M$	$2.3\times10^{-8}\exp(^-24494/T_{gas})$	12
R232	$H + NO + M \rightarrow HNO + M$	$1.5\times10^{-32}\exp(300/T_{gas})$	12
R233	$HNO_3 + O \rightarrow O_2 + HNO_2$	$1.0\times10^{-11}\exp(^-8000/T_{gas})$	12
R234	$HNO_3 + M \rightarrow OH + NO_2 + M$	$2.7\times10^{-9}\exp(^-15400/T_{gas})$	12
R235	$OH + NO_2 + M \rightarrow HNO_3 + M$	1.7×10^{-30}, M= O_2, H_2O	21, 22
R236	$HNO_3 + M \rightarrow H + NO_3 + M$	$2.7\times10^{-9}\exp(^-15400/T_{gas})$	12
R237	$HNO_3 + O \rightarrow OH + NO_3$	$1.0\times10^{-12}\exp(^-4000/T_{gas})$	12
R238	$NO_3 + H \rightarrow NO_2 + OH$	$5.8\times10^{-10}\exp(^-750/T_{gas})$	12
R239	$HNO_3 + OH \rightarrow NO_3 + H_2O$	$1.5\times10^{-14}\exp(650/T_{gas})$	13, 23

R240	$HNO_3 + M \rightarrow OH + NO_2 + M$	$1.83\times10^{-4}(T_{gas}/298)^{-1.98}\exp(-24050/T_{gas})$	12
R241	$HNO_2 + M \rightarrow OH + NO + M$	$2.8\times10^{-9}(300/T_{gas})^{-1}\exp(-25000/T_{gas})$	12
R242	$NO + OH + M \rightarrow HNO_2 + M$	$2.2\times10^{-32}\exp(1000/T_{gas})$	12
R243	$H_2 + NO_2 \rightarrow H + HNO_2$	$4\times10^{-11}\exp(-14500/T_{gas})$	12
R244	$H + HNO_2 \rightarrow H_2 + NO_2$	$1.4\times10^{-11}(300/T_{gas})^{0.5}\exp(-1500/T_{gas})$	12
R245	$O + HNO_2 \rightarrow OH + NO_2$	$1\times10^{-12}\exp(-2000/T_{gas})$	12
R246	$OH + HNO_2 \rightarrow H_2O + NO_2$	$2.5\times10^{-12}\exp(-28/T_{gas})$	12
R247	$H_2O + NO_2 \rightarrow OH + HNO_2$	$1.4\times10^{-12}\exp(-21136/T_{gas})$	12
R248	$O + O_2 + M \rightarrow O_3 + M$	$7.6\times10^{-34}(300/T_{gas})^{1.9}$, M= O_2, NO, NO_2, NO_3	12
		$3.9\times10^{-33}*(300/T_{gas})^{1.9}$, M= N, O	12
		$5.8\times10^{-34}*(300/T_{gas})^{2.8}$ for the rest neutrals	
R249	$N + O_3 \rightarrow NO + O_2$	2×10^{-16}	12
R250	$O_2 + O_2 \rightarrow O_3 + O$	$2\times10^{-11}\exp(-49800/T_{gas})$	12
R251	$O_2 + NO_2 \rightarrow NO + O_3$	$2.8\times10^{-12}\exp(-25400/T_{gas})$	12
R252	$NO_2 + O_3 \rightarrow O_2 + NO_3$	$1.2\times10^{-13}\exp(-2450/T_{gas})$	12
R253	$NO_3 + NO_3 \rightarrow O_2 + 2NO_2$	$4.3\times10^{-12}\exp(-3850/T_{gas})$	12
R254	$O_3 + M \rightarrow O_2 + O + M$	$6.3\exp(170/T_{gas})\times6.6\times10^{-10}\exp(-11600/T_{gas})$, M= N,O	12
		$0.38\times6.6\times10^{-10}\exp(-11600/T_{gas})$, M= O_2	12
		$6.6\times10^{-10}\exp(-11600/T_{gas})$ for the rest neutrals	12
R255	$O_3 + H \rightarrow OH + O_2$	$2.8\times10^{-11}(300/T_{gas})^{0.75}$	12
R256	$OH + O_2 \rightarrow O_3 + H$	$2.7\times10^{-13}(300/T_{gas})^{1.44}\exp(-38600/T_{gas})$	12
R257	$O_3 + OH \rightarrow HO_2 + O_2$	$1.6\times10^{-12}\exp(-1000/T_{gas})$	12
R258	$HO_2 + O_2 \rightarrow O_3 + OH$	1.5×10^{-15}	12
R259	$O_3 + HO_2 \rightarrow OH + 2O_2$	$3.3\times10^{-14}\exp(-1000/T_{gas})$	12
R260	$O_3 + H_2 \rightarrow OH + HO_2$	$1.0\times10^{-13}\exp(-10000/T_{gas})$	12

ǂ All 3-body reactions are in the unit of [cm^6 s^{-1}]

* For newly added species H_2O, O_2, NO and N_2O, the related electron cross section data were retrieved from lxcat.net[24-26] where the different database is cited for the individual species separately. From previous N_2-H_2 model[1], the same built-in electron cross section data of BOLSIG+ (retrieved June 2013) were used for nitrogen and hydrogen species.

⸸ Assumed similar reaction coefficient of ion-ion neutralization coefficient with R42-43

ɸ Assumed similar reaction coefficient with R51-52

Ŧ Hayashi database from lxcat. net provides the combined cross section values of two vibrationally excited states of $H_2O(\nu_1)$ and $H_2O(\nu_3)$ indicated as H_2O(0.459 eV) whereas the bend(010) mode ν_2 as H_2O(0.206 eV). The notation of different vibrational state of H_2O is followed by Buckingham.[18]

ǂ The original reference [27, 28] cited in Kossyi et al.[11] provided the reaction coefficient 1x10^{-11} cm^3 s^{-1} as quenching rate coefficient of $N_2(A3)$ by N_2O which does not explicitly suggested the further dissociation. The impact of this reaction R124 is discussed in SI section 3.

γ (R190) indicates the emitted photon from intermediate excited energy state of NO_2*

Equation S1. V-T interaction coefficient of $N_2(\nu_i)$ by $H_2O(X)$

The rate coefficient k_{10}^{VT} for relaxation of the lowest excited vibrational state is

$$k_{10}^{VT}\ [cm^3s^{-1}] = AT^n\exp\left(-\frac{B}{T^{\frac{1}{3}}}+\frac{C}{T^m}\right)\left[1-D\exp\left(-\frac{E_{10}}{T}\right)\right]^{-1} \qquad (S1)$$

where T is gas temperature in the unit of K. The V–T relaxation coefficient for higher vibrational levels of N_2 ($1\leq\nu\leq8$) is calculated as described in elsewhere[1] following the relation as provided in Capitelli et al.[12]

The values of the parameters in the equation (S1) for V-T rate coefficients k_{10}^{VT} are as follows,[12]

n	m	A	B	C	D
1	0	2.5×10^{-15}	21.18	0	0

Table S2. Surface reactions included in N_2/H_2O plasma model

	Process	Sticking probability γ /energy [eV]	Ref.
Direct surface adsorption of atoms and radicals			
S1	$N + Surf \rightarrow N_{(ad)}$	γ 0.1 (SiO_2), 1 (Ru/MgO)	[1, 29]
S2	$H + Surf \rightarrow H_{(ad)}$	γ 0.01 (SiO_2), 1 (Ru/MgO)	[1, 29]
S3	$O + Surf \rightarrow O_{(ad)}$	γ 0.01 (SiO_2), 1 (Ru/MgO)	⸸
S4	$NH + Surf \rightarrow NH_{(ad)}$	γ 0.01 (SiO_2), 1 (Ru/MgO)	[1, 29]
S5	$NH_2 + Surf \rightarrow NH_{2(ad)}$	γ 0.01 (SiO_2), 1 (Ru/MgO)	[1, 29]
Recombination and further hydrogenation by E-R interaction			
S6	$N + N_{(ad)} \rightarrow N_2 + Surf$	γ 6.0×10^{-4} (SiO_2), 6.0×10^{-3} (Ru/MgO)	[1, 29]
S7	$H + H_{(ad)} \rightarrow H_2 + Surf$	γ 1.5×10^{-4} (SiO_2), 1.5×10^{-3} (Ru/MgO)	[1, 29]
S8	$O + O_{(ad)} \rightarrow O_2 + Surf$	γ 1.5×10^{-4} (SiO_2), 1.5×10^{-3} (Ru/MgO)	⸸
S9	$H + OH_{(ad)} \rightarrow H_2O + Surf$	γ 8.0×10^{-4} (SiO_2), 8.0×10^{-3} (Ru/MgO)	⸸
S10	$N + H_{(ad)} \rightarrow NH_{(ad)}$	γ 1×10^{-3} (SiO_2), 1.0×10^{-2} (Ru/MgO)	[1, 29]
S11	$NH + H_{(ad)} \rightarrow NH_{2(ad)}$	γ 1×10^{-3} (SiO_2), 1.0×10^{-2} (Ru/MgO)	[1, 29]
S12	$NH_2 + H_{(ad)} \rightarrow NH_3 + Surf$	γ 1×10^{-3} (SiO_2), 1.0×10^{-2} (Ru/MgO)	[1, 29]
S13	$H + N_{(ad)} \rightarrow NH_{(ad)}$	γ 8×10^{-4} (SiO_2), 8.0×10^{-3} (Ru/MgO)	[1, 29]
S14	$H + O_{(ad)} \rightarrow OH_{(ad)}$	γ 8×10^{-4} (SiO_2), 8.0×10^{-3} (Ru/MgO)	⸸
S13	$H + NH_{(ad)} \rightarrow NH_{2(ad)}$	γ 8×10^{-4} (SiO_2), 8.0×10^{-3} (Ru/MgO)	[1, 29]
S14	$H + NH_{2(ad)} \rightarrow NH_3$	γ 8×10^{-4} (SiO_2), 8.0×10^{-3} (Ru/MgO)	[1, 29]
S15	$H_2 + NH_{(ad)} \rightarrow NH_3$	γ 8×10^{-5} (SiO_2), 8.0×10^{-4} (Ru/MgO)	[1, 29]
Surface hydrogenation/dehydrogenation by L-H interaction			
S16	$N_{(ad)} + H_{(ad)} \rightarrow NH_{(ad)} + Surf$	N/A (SiO_2), E_a 0.96eV, E_d 0.2 eV (Ru/MgO)	
S17	$NH_{(ad)} + H_{(ad)} \rightarrow NH_{2(ad)} + Surf$	E_a 2.35 eV, E_d 0.5 eV (SiO_2), E_a 1.67eV, E_d 0.2 eV (Ru/MgO)	
S18	$NH_{2(ad)} + H_{(ad)} \rightarrow NH_{3(ad)} + 2Surf$	E_a 3.61 eV, E_d 0.5 eV (SiO_2), E_a 2.06eV, E_d 0.2 eV (Ru/MgO)	
S19	$NH_{3(ad)} + Surf \rightarrow NH_{2(ad)} + H_{(ad)}$	E_a 2.11 eV, E_d 0.9 eV (SiO_2), E_a 1.34 eV, E_d 0.9 eV (Ru/MgO)	This study (SiO_2) [30] (Ru/MgO)
S20	$NH_{2(ad)} + Surf \rightarrow NH_{(ad)} + H_{(ad)}$	E_a 8.0 eV, E_d 0.9 eV (SiO_2), E_a 1.89 eV, E_d 0.9 eV (Ru/MgO)	
S21	$NH_{(ad)} + Surf \rightarrow N_{(ad)} + H_{(ad)}$	N/A (SiO_2), E_a 2.47 eV, E_d 0.9 eV (Ru/MgO)	
Surface adsorption/desorption of NH_3			
S22	$NH_3 + Surf \rightarrow NH_{3(ad)}$	γ 0.2 (SiO_2, Ru/MgO)	[31, 32] §
S23	$NH_{3(ad)} \rightarrow NH_3 + Surf$	E_a 0.61 eV (SiO_2) E_a 0.9 eV (Ru/MgO)	This study (SiO_2) [30] (Ru/MgO)
Dissociative adsorption of N_2, and H_2O			
S24	$N_2 + 2Surf \rightarrow 2N_{(ad)}$	γ 6.7×10^{-9}, E_a 7 eV, E_d 0.9 eV (SiO_2) γ 6.7×10^{-7}, E_a 1.07 eV, E_d 0.9 eV (Ru/MgO)	[33] ǂ
S25	$N_2^* + 2Surf \rightarrow 2N_{(ad)}$	γ 0.001, E_a 7 eV, E_d 0.9 eV (SiO_2) γ 0.1, E_a 1.07 eV, E_d 0.9 eV (Ru/MgO)	This study (SiO_2) [30] (Ru/MgO)
S26	$H_2O + 2Surf \rightarrow H_{(ad)} + OH_{(ad)}$	γ 1×10^{-5}, E_a 0.487, E_d 0.5 eV (SiO_2) γ 1×10^{-3}, E_a 0.5 eV, E_d 0.2 eV (Ru/MgO)	¶ [34](SiO_2) [35] (Ru/MgO)
S27	$H_2 + 2Surf \rightarrow 2H_{(ad)}$	γ 1×10^{-5}, E_a 0.54 eV, E_d 0.5 eV (SiO_2) γ 1×10^{-3}, E_a 0.4 eV, E_d 0.2 eV (Ru/MgO)	¶¶ [36] (SiO_2) [37] (Ru/MgO)

⸸ The sticking probability of direct adsorption of O atoms, E-R interaction between gas phase H and surface adsorbed $O_{(ad)}$ and $OH_{(ad)}$ were assumed to be similar with the interaction of atomic hydrogen species and $N_{(ad)}$, $NH_{x(ad)}$ in the surface reaction of S3, S8, S9 and S14 due to the lack of reference information. For the activation energy of L-H interaction and desorption of $NH_{3(ad)}$ on SiO_2 surface, the calculated values were applied from DFT study as it was discussed in the section of **Underlying mechanism of ammonia production in N_2/H_2O system** of main text. The rest reaction energy values related to nitrogen and hydrogen species were used the same from Hong et al.[1] where the original reaction equations are taken from Carrasco et al.[29] E_a stands for the activation energy of the given surface reaction, E_d is the activation energy for diffusion of surface adsorbed species as defined in Carrasco et al.

§ The same sticking probability γ of NH_3 on Fe surface from Ertl et al.[32] was assumed for Ru/MgO as well as non-catalytic SiO_2 surface due to the lack of relevant data.

ǂ The sticking probability of ground state $N_2(X)$ and vibrationally excited $N_2(\nu_i)$ were calculated by the equation from Hansen et al.[33] where γ 6.7 × 10^{-7} is a calculated value for ground state $N_2(X)$ at T_g 500K on iron-like surface. The activation energy barrier for dissociation of N_2 was calculated in this study for SiO_2 surface and the previous results on Ru/MgO was used for the comparison. The sticking probabilities for electronically-excited states of N_2 were taken the same as those used in Hong et al.[1] The diffusion energy of $N_{(ad)}$ was taken the same as in Hong et al.[1] following Bath.[38]

¶ The sticking probabilities for vibrationally-excited states of H_2O were taken the same as $H_2O(X)$.

¶¶ The sticking probabilities for vibrationally-excited states of H_2O were taken the same as $H_2O(X)$.

2. Calculated diffusion coefficients of important gas phase species in N_2/H_2O system

The binary diffusion coefficient against majority of N_2 molecule are provided in Table S4 based on the collision integral data for interactions between N_2 and species containing nitrogen, hydrogen and oxygen following the methods of calculation.[39,40] For the NH_2-NH_2 interaction, the force constants were obtained using equation (2) of Murphy[40] with X = NH and Y = H. For the H_2O-H_2O interaction, the Stockmayer (12,6,3) potential given by Matsunaga and Nagashima.[41]

Table S3. Calculated binary diffusion coefficient of gas species in N_2/H_2O plasma model [cm^2s^{-1}]

Binary diffusion against N_2	Diffusion coefficient [cm^2s^{-1}]
N_2-N_2	0.66078
N_2-N	0.98086
N_2-H	3.83234
N_2-H_2	2.42681
N_2-NH_3	0.69862
N_2-NH_2	0.75737
N_2-NH	0.83985
N_2-H_2O	0.57616
N_2-O_2	0.76913
N_2-NO	0.65379
N_2-NO_2	0.49392
N_2-N_2O	0.68499
N_2-O	1.17443

3. Influence of spin polarization for DFT calculations

Considering the non-magnetic properties of SiO_2, the spin polarization was not considered in initial calculations from DFT study and the plasma chemistry modelling was performed based on the initial calculation results on activation energy of reaction. However, in order to provide more accurate comparison with Ru/MgO surface condition where the spin polarization is included, the possible impact of spin polarization was examined for the whole procedure of DFT calculations on SiO_2 for NH_3 synthesis. Table S4 shows the results of total energy and enthalpy change under the similar parameters for both with and without the spin polarization effect considered. With the spin polarization effect considered, the calculated total energy of the adsorbed NH_x^* species over SiO_2(001) is much higher than the initial calculation without consideration on the spin polarization. In spite of this difference, except for the hydrogenation step NH^{*}+H(g)→NH_2^*+H^*(-4.479 eV *vs* -3.663 eV), the calculated enthalpy changes between the two modes shows a small difference (<0.2 eV), indicating that the updated calculation with the considered spin polarization may not significantly influence the initial conclusions. The summarized activation energy diagrams are shown in Fig. S1 as a comparison.

Table S4. Comparisons of the total energy and enthalpy change (ΔH) for different calculation parameters.

Adsorption species	Total energy/eV (non-spin-polarized)	ΔH/eV (non-spin-polarized)	Total energy/eV (spin-polarized)	ΔH/eV (spin-polarized)
NH^*	-23897.14899	-	-23898.64846	-
NH^*+H^* (NH^{*}+H(g)→NH^*+H^*)	-23912.42475	-1.65014	-23913.95419	-1.70795
NH_2^* (NH^*+H^*→NH_2^*)	-23913.60217	-1.17722	-23915.22096	-1.26677
$NH_2^*+H^*$ (NH_2^{*}+H(g)→$NH_2^*+H^*$)	-23931.65118	-4.47915	-23932.48143	-3.66270
NH_3^* ($NH_2^*+H^*$→NH_3^*)	-23930.13628	1.51445	-23930.97320	1.50823
NH_3(g) (NH_3^*→NH_3(g))	-23929.52396	0.61232	-23930.42351	0.54969
TS1 (NH^*+H^*→NH_2^*)	-23910.07378	E_a=2.35189	-23911.63507	E_a=2.31912
TS2 ($NH_2^*+H^*$→NH_3^*)	-23928.02290	E_a=3.62813	-23929.02072	E_a=3.46046

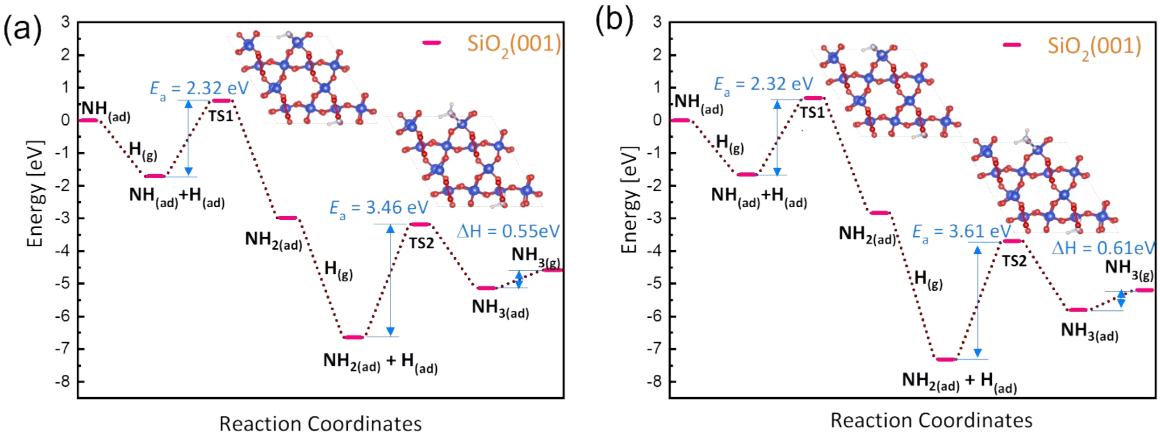

Fig. S1 Influence of spin polarization on DFT calculation result of hydrogenation and dehydrogenation of $NH_{x(ad)}$ and desorption of $NH_{3(ad)}$ on SiO_2 surface: With(a) and without(b) spin polarization considered

Applying these two different set of data on E_a and ΔH for ammonia desorption with and without spin polarization, plasma chemistry model was examined its possible influence for NH_3 production at the standard condition. As shown in Table S5, the calculated density of most of gas and surface adsorbed species remain intact. A small decrease in activation energy to produce $NH_{2(ad)}$ and $NH_{3(ad)}$ by Langmuir-Hinshelwood mechanism as well as increased desorption of $NH_{3(ad)}$ resulted in slight increase in the density of $NH_{2(ad)}$ and decrease in $NH_{3(ad)}$ density. Nevertheless, ammonia production especially in this non-catalytic surface condition proceeds predominantly by Eley-Rideal mechanism[42] so that the overall change in the density of produced ammonia showed only 0.7% of increase with the spin polarization included in DFT study. The most calculation results on different gas composition, power and residence time is considered to be preserved well without significant change.

Table S5. Comparisons of density of important gas phase and surface adsorbed species with and without spin polarization considered in DFT study on SiO_2 surface where constant E/N 82.3 Td, n_e 3.6×10^9 cm^{-3} and T_g 500K assumed as same as Fig. 2, 3 and 6 in the main paper

Gas species	**Without spin polarization** [cm^{-3}]	**With spin polarization** [cm^{-3}]	**Surface species**	**Without spin polarization** [cm^{-2}]	**With spin polarization** [cm^{-2}]
$N_2(v_1)$	9.10×10^{16}	9.10×10^{16}	**Surf**	3.40×10^{13}	3.40×10^{13}
$N_2(v_8)$	1.77×10^{12}	1.77×10^{12}	**$N_{(ad)}$**	3.14×10^{12}	3.14×10^{12}
$N_2(A3)$	2.27×10^{13}	2.26×10^{13}	**$O_{(ad)}$**	5.64×10^{12}	5.67×10^{12}
N	8.18×10^{13}	8.18×10^{13}	**$H_{(ad)}$**	6.50×10^{14}	6.50×10^{14}
H	5.59×10^{14}	5.59×10^{14}	**$OH_{(ad)}$**	2.81×10^{14}	2.81×10^{14}
O	1.55×10^{14}	1.55×10^{14}	**$NH_{(ad)}$**	1.52×10^{13}	1.52×10^{13}
N_2O	2.63×10^{14}	2.65×10^{14}	**$NH_{2(ad)}$**	9.88×10^{12}	9.93×10^{12}
NH_3	6.83×10^{14}	6.88×10^{14}	**$NH_{3(ad)}$**	2.95×10^{9}	6.86×10^{8}

4. Discussion on important production and loss mechanism of N_2O

From the experiment, N_2O was observed as predominant N_xO_y species among other possibilities in N_2/H_2O plasma system. The sensitivity result showed the predominant role of N_2(A3) in production and loss mechanism of N_2O via reaction R123 and R124 as shown in Fig. S2 below. The interaction between nitrogen atom N and NO_2 (R187), also NH_2 and NO_2 (R212) contributed to produce N_2O predominantly. However, the loss rate of N_2O from this single reaction R124, the dissociation of N_2O by N_2(A3), appeared to be excessively high and the maximum reaction rate from the rest loss mechanisms is four orders of magnitude lower. In addition, it is important to note that it was indicated as a quenching rate coefficient of N_2(A3) by N_2O without explicit description of further dissociation of N_2O in the original references[27, 28] cited in Kossyi et al.[11].

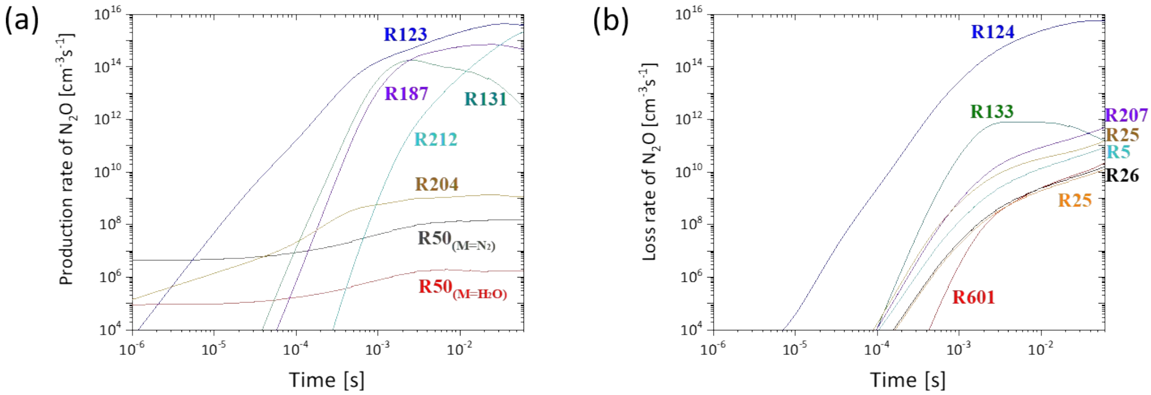

Fig. S2. Important production (a) and loss (b) reaction of N_2O in N_2/H_2O plasma system

Table S6. Important production and loss reactions of N2O and its reaction coefficient as indicated in Fig. S2.

Reaction No in Table S1.	Important production reactions of N_2O	Rate coefficient [cm^3s^{-1}] [cm^6s^{-1}]ǂ
R123	$N_2(A3) + O_2 \rightarrow N_2O + O$	$2.0\times10^{-14}(T_{gas}/300)^{0.55}$ [cm^3s^{-1}]
R187	$N + NO_2 \rightarrow O + N_2O$	3×10^{-12} [cm^3s^{-1}]
R212	$NH_2 + NO_2 \rightarrow N_2O + H_2O$	$2.67\times10^{-8}(T_{gas}/300)^{-1.4}\exp(-135/T_{gas})$ [cm^3s^{-1}]
R131	$N(2D) + NO \rightarrow N_2O$	6×10^{-11} [cm^3s^{-1}]
R204	$O + N_2 + M \rightarrow N_2O + M$	$3.9\times10^{-35}\exp(-10400/T_{gas})$ [cm^6s^{-1}]
R50	$O^- + N_2^+ + M \rightarrow N_2O + M$	$2\times10^{-25}(300/T_{gas})^{2.5}$ [cm^6s^{-1}]

Reaction No in Table S1.	Important loss reactions of N_2O	Rate coefficient
R124	$N_2(A3) + N_2O \rightarrow N_2 + N + NO$	1.0×10^{-11}ǂ [cm^3s^{-1}]
R133	$N(2D) + N_2O \rightarrow NO + N_2$	3×10^{-12} [cm^3s^{-1}]
R207	$N_2O + H \rightarrow N_2 + OH$	$1.3\times10^{-10}\exp(-7600/T_{gas})$ [cm^3s^{-1}]
R5	$e + N_2O \rightarrow e + e + N_2O^+$	BOLSIG+
R151	$N_2O + NH \rightarrow N_2 + HNO$	$3.3\times10^{-12}\exp(-3000/T_{gas})$ [cm^3s^{-1}]
R206	$N_2O + OH \rightarrow N_2 + HO_2$	$1.0\times10^{-12}\exp(-5000/T_{gas})$ [cm^3s^{-1}]

R25	$N_2^+ + N_2O \rightarrow N_2O^+ + N_2$	5.0×10^{-10} [cm^{3}s^{-1}]
R26	$N_2^+ + N_2O \rightarrow NO^+ + N + N_2$	4.0×10^{-10} [cm^{3}s^{-1}]

The density profile of important gas species is compared between two different conditions with the original reaction coefficient k_{R124}1x10^{-11} [cm^{3}s^{-1}] from Kossyi et al.[11] and adjusted lower reaction coefficient value of 1x10^{-13} [cm^{3}s^{-1}] as shown in Fig. S3. Again, it confirmed the significant influence of single reaction of dissociation of N_2O by N_2(A3) which results in approximately a factor of ten increase of N_2O. Considering the experimental observation of no detected NO_x and higher production rate of N_2O than NH_3, the adjusted k_{R124} 1x10^{-13} [cm^{3}s^{-1}] value was taken for all the modelling results shown in this study.

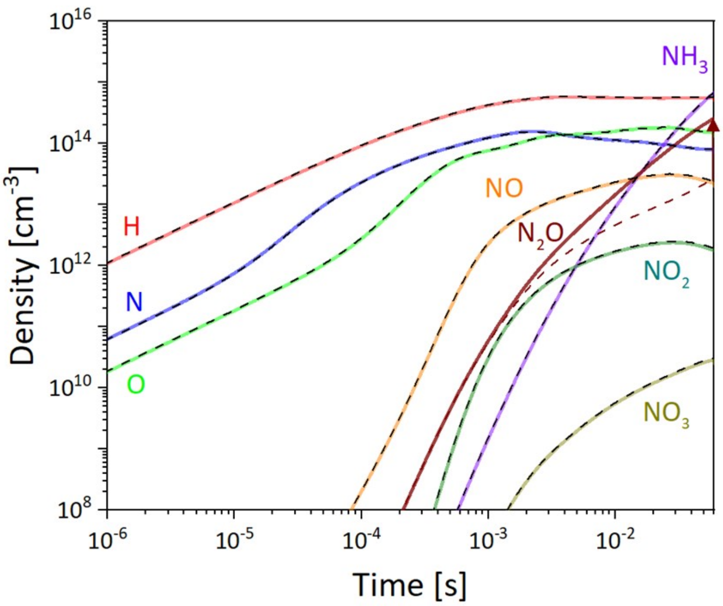

Fig. S3 Comparison of density profile of important gas species with two different dissociation reaction coefficient k_{R124}; coloured solid curve with k_{R124}=1x10^{-13} [cm^{3}s^{-1}] as same as shown in Fig. 2 in main text, dashed curve with k_{R124} =1x10^{-11} [cm^{3}s^{-1}] where, residence time in plasma discharge 0.06 s, constant E/N 82.3 Td, ne 3.6x10^9 cm^{-3} and T_g 500K assumed

As we discussed in the main text, still the estimated density of N_2O is much lower than the measurement. It is considered that a recombination reaction in the remote plasm area can be the reason for this difference. A possible mechanism of N_2O production in the downstream of the burner was suggested by Groves and Sasonow,[43] which is a strongly exothermic reaction between NH_3 and NO as shown below.

$$2NH_3 + 8NO \rightarrow 5N_2O + 3H_2O, \qquad \Delta H = -945.7 \text{ kJ}$$

$$4NH_3 + 4NO + 3O_2 \rightarrow 4N_2O + 6H_2O, \qquad \Delta H = -2403.3 \text{ kJ}$$

Considering the underestimated N_2O by model, it seems to be highly possible to occur in our remote plasma area in between active DBD discharge volume and bulk liquid domain where the gas products are dissolved and collected. However, further investigation may require in order to validify this assumption.

5. Influence of a newly suggested two-step dissociative adsorption in N_2/H_2O Plasma Kinetic Model

The density profile of important gas species was calculated by the conventional method[1] to show the influence in comparison to the newly suggested two-step model of the dissociative adsorption. Figure S4 shows a decrease in the surface adsorbed $N_{(ad)}$ density by adapting new reaction coefficient $k_{diss.ads.}$ while the rest density profiles are remained without any meaningful change. In log time scale, Fig. S4(b) reveals more clearly that the previous model may generate relatively high $N_{(ad)}$ density by overestimated reaction coefficient for the dissociative adsorption especially in early stage. This update in the calculation of $k_{diss.ads.}$ is considered to provide more reasonable temporal behaviour of $N_{(ad)}$ particularly at early stage. As a result, in comparison to the result based on the conventional concept of dissociative adsorption of N_2, this update in the model resulted in 9.4% smaller $N_{(ad)}$ and 1.2% decreased NH_3 concentration at given residence time and plasma condition as shown in summarized Table S5.

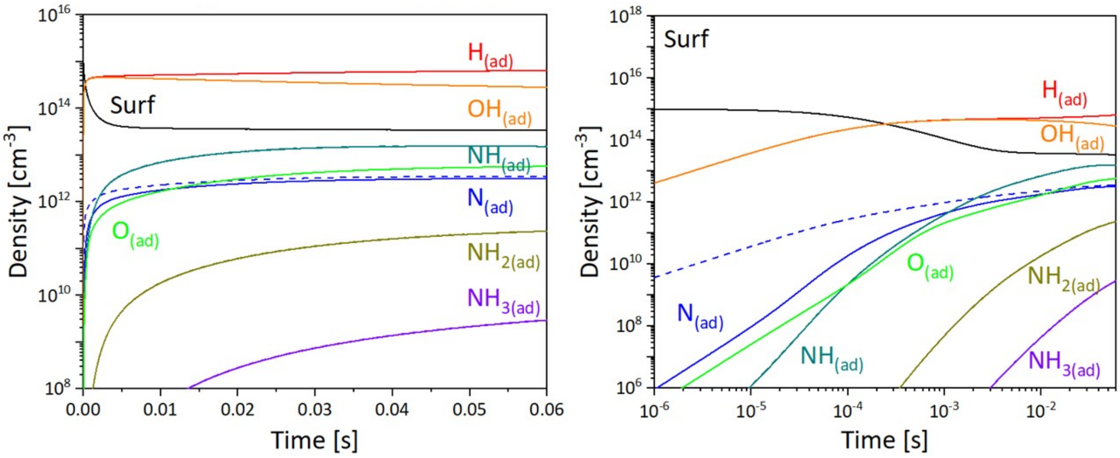

Fig. S4 Comparison of density profile of important surface adsorbed species with $k_{diss.ads.}$ from previous model and new suggestion in this work (a) in linear time scale (b) in log scale where residence time in plasma discharge 0.06 s, constant E/N 82.3 Td, n_e 3.6x10^9 cm^{-3} and T_g 500K assumed

Table S7. Calculated densities of important gas and surface adsorbed species at the same condition as shown in Fig. S4

Dissociative adsorption	N [cm^{-3}]	H [cm^{-3}]	NH [cm^{-3}]	NH_3 [cm^{-3}]	O [cm^{-3}]	$N_{(ad)}$ [cm^{-2}]	$H_{(ad)}$ [cm^{-2}]	$NH_{(ad)}$ [cm^{-2}]
Conventional	8.05x10^{13}	5.47x10^{14}	1.03x10^{11}	6.89x10^{14}	1.53x10^{14}	3.52x10^{12}	6.47x10^{14}	1.56x10^{14}
This model	**8.03x10^{13}**	**5.47x10^{14}**	**1.03x10^{11}**	**6.81x10^{14}**	**1.53x10^{14}**	**3.19x10^{12}**	**6.48x10^{14}**	**1.54x10^{14}**

6. Influence of V-T relaxation of $N_2(\nu_i)$ by H_2O

Increasing density of H_2O in the N_2/H_2O plasma system is important to enable efficient NH_3 production by increased hydrogen source in the discharge and on the surface. However, by the increased H_2O concentration, it quenches the plasma density and energy significantly mainly by vibrational-translational interaction between $N_2(\nu_i)$ and H_2O as summarized in Table S8.

Figure S5 shows the influence of V-T relaxation in the distribution function of vibrationally excited ground state nitrogen molecules $N_2(\nu_i)$ At different gas temperature of 300K and 500K, the calculation suggests that without V-T relaxation of $N_2(\nu_i)$ by H_2O, the population of high-lying vibrationally excited species can be overestimated even higher than N_2/H_2 system. Table S9 provide more parameters for comparison to show the importance of the quenching effect of H_2O. Without consideration on V-T relaxation, the electron temperature and estimated power can be misinterpreted as up to 20466K and 71.6W at the given plasma condition. However, when the quenching effect takes place, the electron temperature and the power was reduced to 12700K and 58W. It resulted in the decreased densities of overall reactive species including atoms, radicals and produced ammonia as well. Therefore, the effect of V-T relaxation can be considered as the most important factor to understand the characteristics of ammonia synthesis from N_2/H_2O plasma system in addition to the loss of nitrogen through the simultaneous oxidation reaction.

Table S8. Comparison of calculated plasma conditions at different H_2O concentration where the same condition of E/N 82.3 Td and T_g 500 K applied.

Concentration of H_2O [%]	**Te** [K]	**Power density** [W cm^{-3}]	**n[N]** [cm^{-3}]	**n[H]** [cm^{-3}]	**n[NH_3]** [cm^{-3}]
0.5%	**13700**	**63.5**	**1.3×10^{14}**	**2.0×10^{14}**	**3.7×10^{14}**
2.0%	**12750**	**58.3**	**8.0×10^{13}**	**5.5×10^{14}**	**6.8×10^{14}**
10.0%	**10460**	**42.2**	**2.8×10^{13}**	**1.7×10^{15}**	**3.7×10^{14}**

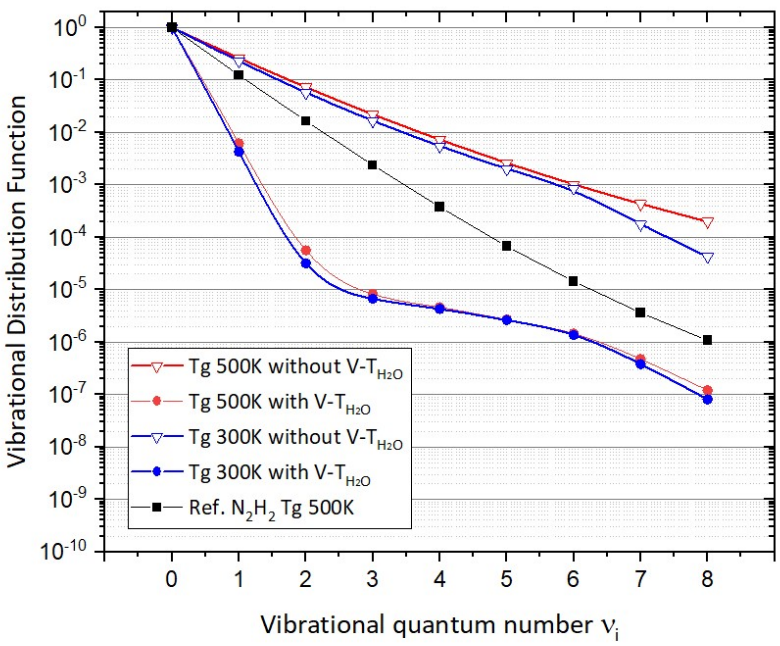

Fig. S5 Comparison of Vibrational distribution function(VDF) with and without V-T relaxation of $N_2(\nu_i)$ by ground state H_2O where the VDF of N_2/H_2 system at the same plasma parameters given as a reference.

Table S9. Calculated densities of important gas and surface adsorbed species at the same condition as shown in Fig. S4

Model	V-T interaction	T_g [K]	T_e [K]	NH_3[cm^{-3}]
N_2/H_2 model	All included V-V, V-V' and V-T	**500**	**16600**	**9.5×10^{15}**
N_2/H_2O model	Without V-T_{H2O} interaction	**500**	**20470**	**2.0×10^{15}**
	With V-T_{H2O} interaction	**500**	**12750**	**6.8×10^{14}**
	Without V-T_{H2O} interaction	**300**	**19920**	**1.0×10^{14}**
	With V-T_{H2O} interaction	**300**	**12790**	**2.3×10^{13}**

References

1. J. Hong, S. Pancheshnyi, E. Tam, J. J. Lowke, S. Prawer and A. B. Murphy, *Journal of Physics D: Applied Physics*, 2017, **50**, 154005.
2. G. J. M. Hagelaar and L. C. Pitchford, *Plasma Sources Sci T*, 2005, **14**, 722-733.
3. Hayashi database, www.lxcat.net, retrieved on 01 Feb., 2021.
4. L.C. Pitchford, B.V. McKoy, A. Chutjian, and S. Trajmar, *Swarm Studies and Inelastic Electron-Molecule Collisions*, Springer-Verlag, New York, 1987
5. PHELPS database, www.lxcat.net, retrieved 04 Jun., 2013
6. S. A. Lawton and A. V. Phelps, *J. Chem. Phys.*, 1978, **69,** 1055.
7. Itikawa database, www.lxcat.net, retrieved 01 Feb., 2021
8. Y. Itikawa, *J. Phys. Chem. Ref. Data* 2016, **45**, 033106.
9. QUANTEMOL database, www.lxcat.net, retrieved 01 Feb., 2021
10. Y. Itikawa and N. Mason, *J. Phys. Chem. Ref. Data*, 2005, **34**, 1.
11. I. A. Kossyi, A. Y. Kostinsky, A. A. Matveyev and V. P. Silakov, *Plasma Sources Sci. Technol.*, 1992, **1,** 207-220.
12. C. F. M. Capitelli, B. Gordiets and A. Osipov, *Plasma Kinetics in Atmospheric Gases*, Springer-Verlag Berlin, 2000.
13. R. Dorai, PhD thesis, University of Illinois at Urbana-Champaign 2002.
14. R. E. Olson, J. R. Peterson and J. Moseley, *The Journal of Chemical Physics*, 1970, **53**, 3391-3397.
15. Y. Sakiyama, D. B. Graves, H.-W. Chang, T. Shimizu and G. E. Morfill, *Journal of Physics D: Applied Physics*, 2012, **45**, 425201.
16. B. M. Z. a. G. A. P. A. N. Yermakov, *International Journal of Radiation Applications and Instrumentation. Part C. Radiation Physics and Chemistry*, 1992, **39**, 455-461.
17. D. S. Stafford and M. J. Kushner, *Journal of Applied Physics*, 2004, **96**, 2451-2465.
18. A. D. Buckingham, *Journal of Molecular Structure*, 1991, **250**, 111-118.
19. B. F. Gordiets, C. M. Ferreira, V. L. Guerra, J. M. A. H. Loureiro, J. Nahorny, D. Pagnon, M. Touzeau and M. Vialle, *IEEE Transactions on Plasma Science*, 1995, **23**, 750-768.
20. K. P. Shrestha, L. Seidel, T. Zeuch and F. Mauss, *Energy & Fuels*, 2018, **32**, 10202-10217.
21. IST Chemical Kinetics Database, Standard Reference Database 17, Version 7.0 (Web Version), Release 1.6.8 Data Version 2013.03.
22. S. Norberg, PhD thesis, University of Michigan, 2015.
23. S. Mukkavilli, C. K. Lee, K. Varghese and L. L. Tavlarides, *IEEE Transactions on Plasma Science*, 1988, **16**, 652-660.
24. E. Carbone, W. Graef, G. Hagelaar, D. Boer, M. M. Hopkins, J. C. Stephens, B. T. Yee, S. Pancheshnyi, J. van Dijk and L. Pitchford, *Atoms*, 2021, **9**.
25. S. Pancheshnyi, S. Biagi, M. C. Bordage, G. J. M. Hagelaar, W. L. Morgan, A. V. Phelps and L. C. Pitchford, *Chemical Physics*, 2012, **398**, 148-153.
26. L. C. Pitchford, L. L. Alves, K. Bartschat, S. F. Biagi, M.-C. Bordage, I. Bray, C. E. Brion, M. J. Brunger, L. Campbell, A. Chachereau, B. Chaudhury, L. G. Christophorou, E. Carbone, N. A. Dyatko, C. M. Franck, D. V. Fursa, R. K. Gangwar, V. Guerra, P. Haefliger, G. J. M. Hagelaar, A. Hoesl, Y. Itikawa, I. V. Kochetov, R. P. McEachran, W. L. Morgan, A. P. Napartovich, V. Puech, M. Rabie, L. Sharma, R. Srivastava, A. D. Stauffer, J. Tennyson, J. de Urquijo, J. van Dijk, L. A. Viehland, M. C. Zammit, O. Zatsarinny and S. Pancheshnyi, *Plasma Processes and Polymers*, 2017, **14**, 1600098.
27. G. Black, T. G. Slanger, G. A. St. John and R. A. Young, *The Journal of Chemical Physics*, 1969, **51**, 116-121.

28. G. W. Taylor and D. W. Setser, *Journal of the American Chemical Society* 1971, **93**, 4930-4932.
29. E. Carrasco, M. Jiménez-Redondo, I. Tanarro and V. J. Herrero, *Physical Chemistry Chemical Physics*, 2011, **13**, 19561-19572.
30. T. Zhang, R. Zhou, S. Zhang, R. Zhou, J. Ding, F. Li, J. Hong, L. Dou, T. Shao, A. B. Murphy, K. Ostrikov and P. J. Cullen, *ENERGY & ENVIRONMENTAL MATERIALS*, 2021, **0**, 1-9.
31. L. R. Winter, B. Ashford, J. Hong, A. B. Murphy and J. G. Chen, *ACS Catalysis*, 2020, **10**, 14763-14774.
32. G. Ertl, *Catalysis Reviews*, 1980, **21**, 201-223.
33. F. Y. Hansen, N. E. Henriksen, G. D. Billing and A. Guldberg, *Surface Science*, 1992, **264**, 225-234.
34. J. Narayanasamy and J. D. Kubicki, *The Journal of Physical Chemistry B*, 2005, **109**, 21796-21807.
35. A. Michaelides, A. Alavi and D. A. King, *Journal of the American Chemical Society*, 2003, **125**, 2746-2755.
36. H. A. Kurtz and S. P. Karna, *The Journal of Physical Chemistry A*, 2000, **104**, 4780-4784.
37. M. Puisto, H. Nenonen, A. Puisto and M. Alatalo, *The European Physical Journal B*, 2013, **86**, 396.
38. J. V. Barth, *Surface Science Reports*, 2000, **40**, 75-149.
39. A. B. Murphy, *Chemical Physics*, 2012, **398**, 64-72.
40. A. B. Murphy, *Plasma Chemistry and Plasma Processing*, 1995, **15**, 279-307.
41. N. Matsunaga and A. Nagashima, *Journal of Physical Chemistry*, 1983, **87**, 5268-5279.
42. Y. Engelmann, K. van 't Veer, Y. Gorbanev, E. C. Neyts, W. F. Schneider and A. Bogaerts, *Acs Sustain Chem Eng*, 2021, **9**, 13151-13163.
43. M. C. E. Groves and A. Sasonow, *Journal of Integrative Environmental Sciences*, 2010, **7**, 211-222.